ARTICLE
Journal of Cellular Biochemistry 117:247–258 (2016)

Journal of Cellular Biochemistry

Stimulation of Cell Migration by Flagellin Through the p38 MAP Kinase Pathway in Cultured Intestinal Epithelial Cells

Yutaka Kondo,[1,2*] Sayomi Higa-Nakamine,[2] Noriko Maeda,[2] Seikichi Toku,[2] Manabu Kakinohana,[3] Kazuhiro Sugahara,[3] Ichiro Kukita,[1] and Hideyuki Yamamoto[2]

[1]*Department of Emergency Medicine, Graduate School of Medicine, University of the Ryukyus, Okinawa 903-0215, Japan*

[2]*Department of Biochemistry, Graduate School of Medicine, University of the Ryukyus, Okinawa 903-0215, Japan*

[3]*Department of Anesthesiology, Graduate School of Medicine, University of the Ryukyus, Okinawa 903-0215, Japan*

ABSTRACT

Toll-like receptor 5 (TLR5) is a receptor for flagellin and is present on the basolateral surface of intestinal epithelial cells. However, the pathological roles of TLR5 in intestinal epithelial cells are not clear at present. In previous reports, we demonstrated that treatment of cultured alveolar epithelial cells with flagellin activated the p38 mitogen-activated protein kinase (MAPK) pathway and enhanced epithelial-mesenchymal transition induced by transforming growth factor beta 1 (TGF-β1). In translating our findings in alveolar epithelial cells to intestinal epithelial cells, we found that both flagellin and TGF-β1 activated p38 MAPK and its downstream protein kinase, MAPK-activated protein kinase-2 (MAPKAPK-2) in an IEC-6 intestinal epithelial cell line. The phosphorylation of HSP27, one of the substrates for MAPKAPK-2, was also increased. TGF-β1 increased the protein level of α-smooth muscle actin (αSMA), and flagellin enhanced the effect of TGF-β1. A wound healing assay revealed that flagellin and TGF-β1 stimulated the migration of cells. SB203580, an inhibitor of p38 MAPK, and an inhibitor of MAPKAPK-2 inhibited flagellin-stimulated migration. These results suggested that TLR5 is involved in the migration of intestinal epithelial cells through activation of the p38 MAPK pathway. J. Cell. Biochem. 117: 247–258, 2016.

KEY WORDS: FLAGELLIN; IEC-6 CELLS; INTESTINAL EPITHELIAL CELLS; MIGRATION; p38 MAPK; TLR5

Flagellin, a primary structural component of bacterial flagella, is generally considered to be one of several pathogen-associated molecular patterns (PAMPs). Toll-like receptor 5 (TLR5) is the receptor for flagellin in vertebrates [Hayashi et al., 2001] and is present on cell membranes, such as the basolateral surface of intestinal epithelial cells [for review, see Ref. Zeng et al., 2006]. TLR5 reportedly recognizes 13 amino acid residues in flagellin that are buried and not accessible in polymerized flagellar filaments [Smith et al., 2003]. It is well known that stimulation of TLR5 by flagellin in intestinal epithelial cells activates the gene expression of pro-inflammatory cytokines such as interleukin-8 (IL-8) [Zeng et al., 2006; for review, see Ref. Sierro et al., 2001]. Microarray analysis of intestinal epithelial cell lines revealed that TLR5 stimulation induced gene expression of anti-apoptotic factors and pro-inflammatory cytokines [Zeng et al., 2006]. Despite all of the data concerning the effects of flagellin on inflammation in the intestine, the pathological roles of TLR5 other than inflammation have not been fully explored.

The authors declare that no significant conflicts of interest exist with any companies/organizations whose products or services may be discussed in this article.

Abbreviations: CD, Crohn's disease; CHOP, CCAAT-enhancer-binding protein homologue protein; DMEM, Dulbecco's modified Eagle's medium; EGFR, epidermal growth factor receptor; EMT, epithelial-mesenchymal transition; ERK, extracellular signal-regulated kinase; FCS, fetal calf serum; GAPDH, glyceraldehyde-3-phosphate dehydrogenase; HSP27, heat shock protein 27; JNK, c-jun N-terminal kinase; MAPK, mitogen-activated protein kinase; MAPKAPK-2, MAPK-activated protein kinase-2; NF-κB, nuclear factor-κB; PBS, phosphate-buffered saline; SE, standard error; αSMA, α-smooth muscle actin; TGF-β1, transforming growth factor beta 1; TLR5, Toll-like receptor 5; TTBS, Tris-buffered saline with Tween-20.

Grant sponsor: JSPS KAKENHI; Grant numbers: 23500451, 24700381, 23390376, 725293329.

*Correspondence to: Yutaka Kondo, MD, Department of Emergency Medicine, Graduate School of Medicine, University of the Ryukyus, 207 Uehara, Nishihara, Okinawa 903-0215, Japan.
E-mail: kondokondou2000@yahoo.co.jp

Manuscript Received: 9 April 2015; Manuscript Accepted: 22 June 2015

Accepted manuscript online in Wiley Online Library (wileyonlinelibrary.com): 24 June 2015

DOI 10.1002/jcb.25272 • © 2015 Wiley Periodicals, Inc.

TLR5 stimulation in alveolar epithelial cells may have a critical role in the onset of Legionella pneumonia [Newton et al., 2010]. In a previous study, we found that stimulation of TLR5 in cultured alveolar epithelial cells enhanced epithelial-mesenchymal transition (EMT) induced by transforming growth factor beta 1 (TGF-β1) [Kondo et al., 2012]. We also found that activation of the p38 mitogen-activated protein kinase (MAPK) pathway was involved in this effect [Kondo et al., 2012].

Crohn's disease (CD) is a disorder of chronic and transmural inflammation [for review, see Ref. Flier et al., 2010]. Dysregulation of wound healing after inflammation may induce a number of complications of CD, including fistula formation. It was suggested that flagellin from commensal gut bacteria initiated an inappropriate immune response in CD, because genetically susceptible individuals had a leaky bowel mucosa, and TLR5 in the basolateral surface of intestinal epithelial cells was activated abnormally [Sun et al., 2007; for review, see Ref. Lodes et al., 2004]. From these reports, we considered the possibility that abnormal overstimulation of TLR5 might affect the functions of intestinal epithelial cells through activation of the p38 MAPK pathway.

IEC-6 cells are immortalized rat intestinal epithelial cells. In the present study, we found that treatment of IEC-6 cells with flagellin activated the p38 MAPK pathway and enhanced the expression of αSMA by TGF-β1. In addition, the effects of flagellin on the EMT and on the migration of IEC-6 cells were examined.

MATERIALS AND METHODS

MATERIALS

The following chemicals and reagents were obtained from the indicated sources: Dulbecco's modified Eagle's medium (DMEM) and phosphate-buffered saline (PBS) from Sigma Chemical Co. (St. Louis, MO); fetal calf serum (FCS) from HyClone (Logan, UT). Antibodies were obtained from several sources: anti-E-cadherin, anti-heat shock protein 27 (HSP27) mouse monoclonal (G31), anti-IκBα, anti-phospho-IκBα (Ser32/36) mouse monoclonal (5A5), anti-MAPKAPK-2 rabbit polyclonal, anti-phospho-MAPKAPK-2 (Thr222) rabbit monoclonal (9A7), anti-phospho-MAPKAPK-2 (Thr334) rabbit monoclonal (27B7), anti-p38 MAPK, anti-phospho-p38 MAPK, anti-SMAD1, anti-SMAD2, anti-SMAD3, anti-phospho-SMAD1, anti-phospho-SMAD2, anti-phospho-SMAD3, anti-rodent HSP27 rabbit polyclonal, and anti-phospho-HSP27 (Ser82) rabbit monoclonal (D1H2) antibodies from Cell Signaling Technology (Beverly, MA); anti-GAPDH antibody from Sigma (St. Louis, MO); anti-fibronectin and anti-α-smooth muscle actin (αSMA) mouse monoclonal antibodies from Abcam (Cambridge, UK); anti-epidermal growth factor receptor (EGFR) mouse monoclonal antibody (6F1) from Assay Designs (Ann Arbor, MI); and anti-phospho-EGFR (Ser1047) mouse monoclonal (anti-P-Ser1047 EGFR antibody) antibody from Acris Antibodies Inc. (San Diego, CA). In addition, an NF-κB luciferase reporter gene (pNF-κB-Luc) was from Stratagene Co. (La Jolla, CA), recombinant human TGF-β1 from R&D Systems Inc. (Minneapolis, MN); SB203580 [4-(4-fluorophenyl)-2-(4-methylsulfinylphenyl)-5-(4-pyridyl) 1H-imidazole] and MK2a inhibitor [4-(2′-fluorobiphenyl-4-yl)-N-(4-hydroxyphenyl)-butyramide] from Calbiochem (Darmstadt, Germany); LDN193189 [4-(6-(4-(piperazin-1-yl) phenyl) pyrazolo[1,5-a]pyrimidin-3-yl) quinoline] and ALK5 inhibitor from Wako Pure Chemical Industries (Osaka, Japan); SMAD3 inhibitor (SIS3) from Merck Millipore Corporation (Darmstadt, Germany); and purified flagellin from *Bacillus subtilis* from InvivoGen (San Diego, CA). Other chemicals were of analytical grade.

CELL CULTURE, TRANSFECTION OF THE LUCIFERASE REPORTER GENE, AND THE DUAL-LUCIFERASE REPORTER GENE ASSAY

IEC-6 cells were obtained from the American Tissue Culture Collection (ATCC) (Manassas, VA) and A549 cells were kindly provided by Dr. Y. Isohama of Tokyo University of Science (Tokyo, Japan). The cells were grown in Petri dishes (Nunc, Roskilde, Denmark) in DMEM containing 4.5 g/l glucose and 10% (vol/vol) heat-inactivated FCS. The firefly-luciferase reporter gene, which has five tandem repeats of the κB-motif (TGGGGACTTTCCGC) upstream of the TATA-box, was transfected into IEC-6 cells. To account for the variation in transfection efficiency among culture dishes, the cells were cotransfected with phRL-TK (Promega Co. WI), which contains the thymidine kinase promoter from the herpes simplex virus to provide constitutive expression of *Renilla* luciferase. IEC-6 cells in 35 mm Petri dishes were cotransfected with pNF-κB-Luc (2.0 μg plasmid DNA) and phRL-TK (0.2 μg plasmid DNA) using 4 μl FuGENE HD transfection reagent (Roche Molecular Biochemicals, Indianapolis, IN, USA) in 2 ml standard medium [Mizutani et al., 2010]. Then, the cells were further cultured for 36–42 h. The medium was exchanged to DMEM containing 0.1% FCS, and the cells were cultured for 1–2 h. The cells were then treated with 2 μg/ml flagellin and/or 10 ng/ml TGF-β1 for the indicated time intervals. The activities of firefly luciferase and *Renilla* luciferase were measured using a Dual-Luciferase Reporter Assay System (Promega Co.) with a luminometer (GLOMAX 20/20) (Promega, Co.) in accordance with the manufacturer's instructions. The ratio of the luminescence from the reaction mediated by firefly luciferase to that from the reaction mediated by *Renilla* luciferase was determined. We noticed that the levels of NF–κB promoter activity in untreated control varied among the experiments. The reasons for this variation were not clear but may be due to differences in cell passage and cell batches [Kondo et al., 2012]. Therefore, representative results are shown instead of the mean ± SE values for all repetitions of identical experiments.

PREPARATION OF CELL EXTRACTS

IEC-6 cells and A549 cells in 60 mm Petri dishes were washed once in PBS and lysed in 300 μL of 1 × SDS–PAGE sample buffer containing 2% (wt/vol) SDS, 62.5 mM Tris-HCl, pH 6.8, 5% (vol/vol) 2-mercaptoethanol, 5% (vol/vol) glycerol, and 0.01% (wt/vol) bromophenol blue [Laemmli, 1970]. The cell extract was sonicated for 20 sec on ice, heated at 98°C for 5 min. The cell extract was kept at −80°C until use [Higa-Nakamine et al., 2012]. We confirmed previously that proteolysis and dephosphorylation of the proteins of interest did not occur during these procedures [Higa-Nakamine et al., 2012; Kondo et al., 2012].

SDS–PAGE AND IMMUNOBLOTTING ANALYSIS

SDS-PAGE was performed by the method of Laemmli [Laemmli, 1970] followed by immunoblotting analysis [Towbin et al., 1979;

Mizutani et al., 2010]. Immunoreactive proteins were detected using an enhanced chemiluminescence detection kit (GE Healthcare UK Ltd, Little Chalfont, UK) and an ImageQuant LAS 4000 mini (GE Healthcare UK Ltd.) with Image Reader LAS 4000 mini (version 1.0; Fuji Film, Japan) in accordance with the manufacturer's instructions. The level of immunoreactivity was quantified using Multi Gauge (version 3.1; Fuji Film, Japan). For reprobing, the membrane was incubated with stripping buffer [62.5 mM Tris-HCl, pH 6.7, 100 mM 2-mercaptoethanol and 2% (wt/vol) SDS] at 50°C for 30 min [Yamanaka et al., 2007]. The membrane was then washed with blocking solution [5% (wt/vol) skim milk, 100 mM Tris-HCl, pH 7.5, 0.9% (wt/vol) NaCl, and 0.1% (vol/vol) Tween-20] followed by Tris-buffered saline with Tween-20 (TTBS) [100 mM Tris-HCl, pH 7.5, 0.9% NaCl, and 0.1% Tween-20] at room temperature, and subjected to immunoblotting analysis.

DETECTION OF ACTIVATION OF THE p38 MAPK PATHWAY

Activation of the p38 MAPK pathway was detected using a GAL4-CHOP assay using the PathDetect in vivo signal transduction pathway *trans*-reporting system (Stratagene Co., La Jolla, CA) [Kondo et al., 2012]. The principle of this system is as follows: the fusion *trans*-activator protein, which consists of the activation domain of the CCAAT-enhancer-binding protein homologue protein (CHOP) fused with the DNA-binding domain of yeast GAL4 (residues 1–147), was expressed in cells by transfection with the pFA-CHOP plasmid. The pFR-Luc reporter plasmid contained a synthetic promoter with five tandem repeats of the yeast GAL4 binding site that control expression of the firefly luciferase gene. Phosphorylation of the activation domain of CHOP by p38 MAPK activates transcription of the firefly-luciferase gene in pFR-Luc. Because CHOP is specifically phosphorylated by p38 MAPK, the level of firefly luciferase activity reflects the activation status of the p38 MAPK pathway in cells. In the experiment, IEC-6 cells in a 35-mm Petri dish were cotransfected with pFA-CHOP (50 ng of plasmid DNA), pFR-Luc (2.0 μg of plasmid DNA), and phRL-TK (0.2 μg of plasmid DNA), as described above. Then, the cells were cultured for a further 24 h. The medium was exchanged for DMEM containing 0.1% FCS, and the cells were cultured for 2 h. The cells were then treated with 2 μg/ml flagellin, 10 ng/ml TGF-β1, or flagellin plus TGF-β1 for 6 h. The activities of firefly luciferase and *Renilla* luciferase were measured as described above.

WOUND HEALING ASSAY

IEC-6 cells and A549 cells were seeded in 24-well plates at 2.5×10^5 cells/well in triplicate. After overnight culture, the culture medium was changed to DMEM containing 0.1% FCS. Wounds were made by scraping a plastic pipette tip across the cell monolayer, and then the wounded cells were cultured with 10 ng/ml TGF-β1 and/or 2 μg/ml flagellin in the presence or absence of 5 μM SB203580 or 20 μM MK2a inhibitor for 24 h. Phase contrast images were recorded at the time of wounding (0 h), 16 h, 24 h, and 48 h using an EVOS f1 (Advanced Microscopy Group, Bothell, WA, USA). Wound areas were quantified using Multi Gauge (version 3.1; Fuji Film, Japan). Wound healing was estimated as a percentage of the remaining wound area relative to the initial wound area [Bakin et al., 2002]. Experiments were repeated three times, and representative results are shown. We noticed that the levels of wound healing in untreated controls varied among the experiments. The reasons for this variation were not clear but may be due to differences in cell passage and cell batches.

CELL GROWTH ASSAY

Cell growth assay was performed using a Cell Counting Kit-8 (Dojin, Kumamoto, Japan) in accordance with the manufacturer's instructions. IEC-6 cells were seeded in 96-well plates at 10,000, 5,000, or 1,000 cells/well in four replicates. After overnight culture, the culture medium was changed to DMEM containing 0.1% FCS, and then the cells were cultured with 10 ng/ml TGF-β1 and/or 2 μg/ml flagellin for 24 h. After 24 h culture, 10 μL of WST-8 was added to each well, and the cells were incubated for an additional 2 h. After incubation, the absorbance at 450 nm was measured using a Microplate Reader (SH-100, Corona Electric, Japan). Cell growth was expressed as a percentage of the absorbance obtained in treated cells relative to that in control cells seeded at 10,000 cells/well.

OTHER PROCEDURES

Protein concentrations were determined using a Qubit Protein Assay Kit with a Qubit 2.0 Fluorometer (Invitrogen, Carlsbad, CA). In pilot experiments, the protein concentration curves were linear in the presence of 0.04% (wt/vol) SDS, 0.1% (vol/vol) 2-mercaptoethanol, and 0.1% (vol/vol) glycerol. Therefore, we diluted the cell extract 50-fold with water for protein quantification. The experiments were repeated at least three times, and representative results are shown. The values are expressed as the mean ± standard error (SE). Statistical analysis was performed using a one-way ANOVA plus Duncan's multiple range test with StatView (version 5.0). $P < 0.05$ was considered statistically significant. In every experiment on luciferase assay and wound healing assay, we used more than three dishes for each condition. In each experiment, we performed statistical analysis to confirm the significance.

RESULTS

ACTIVATION OF THE NF-κB PATHWAY IN IEC-6 CELLS BY FLAGELLIN

It has been reported that flagellin activates the NF-κB pathway in various cell lines [Hayashi et al., 2001; Akira, 2003]. Therefore, we first examined the effects of flagellin on the NF-κB pathway in IEC-6 cells to confirm that IEC-6 cells respond to flagellin (Figs. 1A and 1B). In a previous study with A549 cells, we found that the optimum concentrations required for TGFβ-1 and flagellin to affect cell functions were 10 ng/ml and 2 μg/ml, respectively [Kondo et al., 2012; Noguchi et al., 2013]. Therefore, we treated IEC-6 cells with TGF-β1 or flagellin at these concentrations and examined the phosphorylation of IκBα and NF-κB-mediated transcription. Immunoblotting using an antibody against phospho-IκBα demonstrated that 30 min of treatment with flagellin increased the phosphorylation of IκBα by approximately 10-fold (Fig. 1A). In contrast, no increase in the phosphorylation of IκBα by TGF-β1 and no augmentation of the flagellin effect by TGF-β1 were observed. We then examined changes in the protein level of IκBα using an anti-IκBα antibody. After treatment with flagellin, the protein level

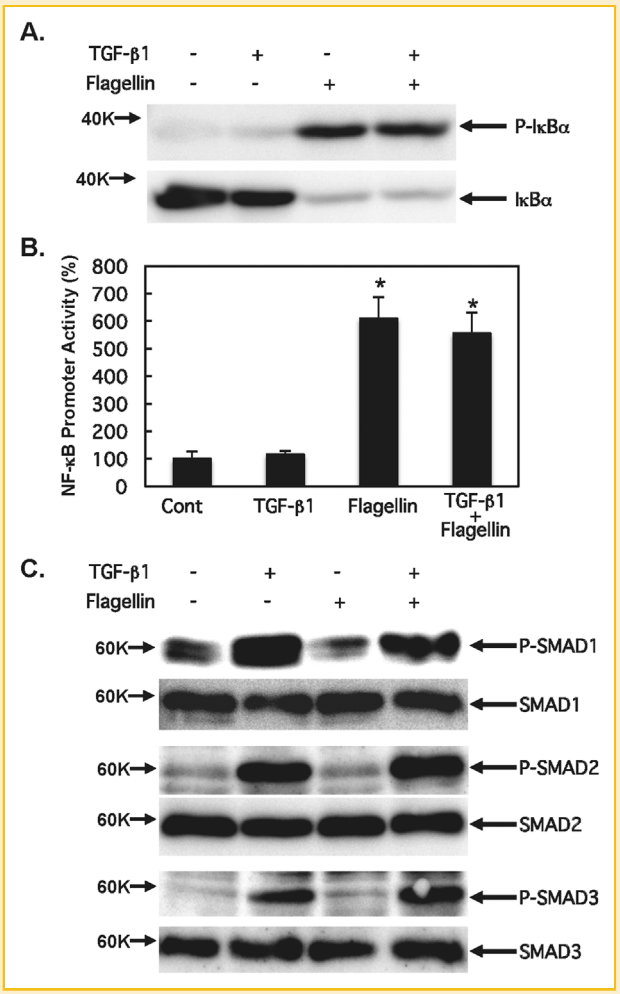

Fig. 1. Effects of transforming growth factor beta 1 (TGF-β1) and flagellin on the nuclear factor-κB (NF-κB) pathway (A, B) and the SMAD pathway (C). *A*: IEC-6 cells were treated with 10 ng/ml TGF-β1, 2 μg/ml flagellin, or both TGF-β1 and flagellin for 30 min. Cell extracts (39.8 μg) were subjected to SDS-PAGE in 10% (wt/vol) acrylamide, and immunoblotting analysis was performed using an anti-phospho-IκBα (1: 2,000) antibody. After the anti-phospho-IκBα antibody was stripped off, immunoblotting with an anti-IκBα antibody was performed at a dilution of 1:2,000. The bands for phospho-IκBα (P-IκBα) and IκBα are indicated. *B*: IEC-6 cells were cotransfected with pNF-κB-Luc (2.0 μg) and phRL-TK (0.2 μg) for 36 h. The cells were treated with 10 ng/ml TGF-β1, 2 μg/ml flagellin, or both TGF-β1 and flagellin for 6 h. The activity without TGF-β1 and flagellin (Cont) was taken to be 100%, and the other values were calculated from this value. Values are the mean ± SE (three samples per condition). $^*P < 0.05$ (vs. control). *C*: IEC-6 cells were treated with 10 ng/ml TGF-β1, 2 μg/ml flagellin, or both TGF-β1 and flagellin for 30 min. The cell extracts (26 μg) were subjected to SDS-PAGE in 10% acrylamide, and immunoblotting analysis was performed with anti-phospho-SMAD1 (1:750), anti-phospho-SMAD2 (1:750), and anti-phospho-SMAD3 (1:750) antibodies. After each antibody was stripped off, immunoblotting with anti-SMAD1 (1:750), anti-SMAD2 (1:750), and anti-SMAD3 (1:750) antibodies, respectively, was performed. Each experiment was repeated two or three times with reproducible results, and representative results are shown.

was decreased to about 13% of the control, indicating the degradation of IκBα after phosphorylation. As expected, no change in the protein level of IκBα in response to TGF-β1 was observed.

NF-κB promoter activity increased to 610.0 ± 76.5% ($P < 0.05$) of the control value after 6 h of treatment with flagellin (Fig. 1B). TGF-β1 did not activate the NF-κB promoter (116.8 ± 12.2%), and no additive effect of flagellin and TGF-β1 was observed (555.9 ± 74.8%). These results indicated that flagellin, but not TGF-β1, activated the NF-κB pathway in IEC-6 cells.

ACTIVATION OF THE SMAD PATHWAY IN IEC-6 CELLS BY TGF-β1

In addition to the NF-κB pathway, we examined the effects of TGF-β1 and flagellin on the SMAD pathway. Phosphorylation of SMAD1, SMAD2, and SMAD3 was increased by approximately 3.4-, 4.1-, and 2.0-fold, respectively, after 30 min of treatment with TGF-β1 (Fig. 1). In contrast, flagellin did not increase the phosphorylation of any SMAD proteins, and no augmentation of the TGF-β1 effect by flagellin was observed. When antibodies against SMAD1, SMAD2, or SMAD3 were used for immunoblotting, no significant changes in immunoreactivity were observed with any treatment (Fig. 1). These results suggested that TGF-β1, but not flagellin, activated the canonical SMAD pathway. From experiments on the activation of the NF-*k*B and SMAD pathways, we confirmed that IEC-6 cells responded to flagellin and TGF-β1. These results indicated also that TLR5 and TGF-β family receptors were signaling distinctly in response to flagellin and TGF-β1, respectively.

ACTIVATION OF THE p38 MAPK PATHWAY IN IEC-6 CELLS BY TGF-β1 AND FLAGELLIN

Flagellin was reported to activate p38 MAPK in T84 intestinal epithelial cells [Harrison et al., 2008]. We reported previously that p38 MAPK was activated by flagellin in two lung epithelial cell lines, A549 and BEAS-2B cells [Kondo et al., 2012]. The activation of p38 MAPK was the greatest among the three MAPKs tested (extracellular signal regulated kinase [ERK], c-jun N-terminal kinase [JNK] and p38 MAPK) [Kondo et al., 2012]. Therefore, we next examined the activation of the p38 MAPK pathway to confirm that IEC-6 cells responded to flagellin (Fig. 2). Immunoblotting using an antibody against phospho-p38 MAPK demonstrated that 30 min of treatment with TGF-β1 and flagellin activated p38 MAPK by approximately 1.5- and 1.8-fold, respectively (Fig. 2A). In addition, p38 MAPK was activated by TGFβ-1 plus flagellin by approximately 2.6-fold, indicating that it was activated in an additive fashion. When an antibody against p38 MAPK was used for immunoblotting, no significant change in immunoreactivity was observed with any treatment (Fig. 2A).

We next examined whether or not the p38 MAPK pathway was activated by TGF-β1 and flagellin using a GAL4-CHOP assay (Fig. 2B). The p38 MAPK pathway was activated by 171 ± 38.7%, 135.5 ± 9.7% ($P < 0.05$), and 193.5 ± 32.3% of the control value by TGF-β1, flagellin, and TGF-β1 plus flagellin, respectively. These results suggested that flagellin activated p38 MAPK and induced the phosphorylation of CHOP by p38 MAPK. Although TGF-β1 appeared to activate the p38 MAPK pathway, activation levels varied among the experiments, and a statistically significant difference between TGF-β1 and the control was not observed.

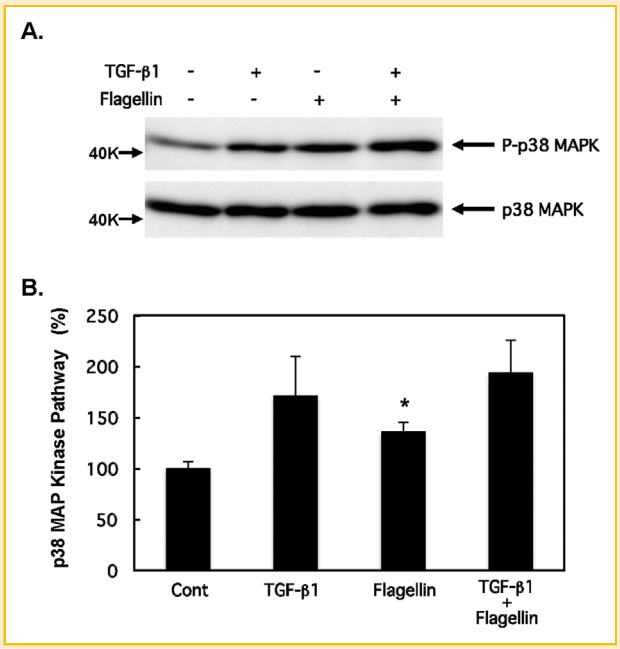

Fig. 2. Activation of p38 mitogen-activated protein kinase (MAPK) and the p38 MAPK pathway by transforming growth factor beta 1 (TGF-β1) and flagellin. A: IEC-6 cells were treated with 10 ng/ml TGF-β1, 2 μg/ml flagellin, or both TGF-β1 and flagellin for 30 min. The cell extracts (39.8 μg) were subjected to SDS-PAGE in 10% (wt/vol) acrylamide, and immunoblotting analysis was performed with an anti-phospho-p38 MAPK antibody (1:750). After the antibody was stripped off, immunoblotting with an anti-p38 MAPK antibody (1:750) was performed. The bands for p38 MAPK (P-p38 MAPK and p38 MAPK) are indicated. B: IEC-6 cells were cotransfected with pFA-CHOP, pFR-Luc, and phRL-TK for 24 h as described in the Materials and Methods. The cells were treated with or without 10 ng/ml TGF-β1, 2 μg/ml flagellin, or both TGF-β1 and flagellin for 6 h. The activity without TGF-β1 and flagellin (Cont) was taken as 100%, and the other values were calculated from this value. Values are the mean ± SE (three samples per condition). $^{*}P < 0.05$ (vs. control). The experiment was repeated three times with reproducible results, and representative results are shown.

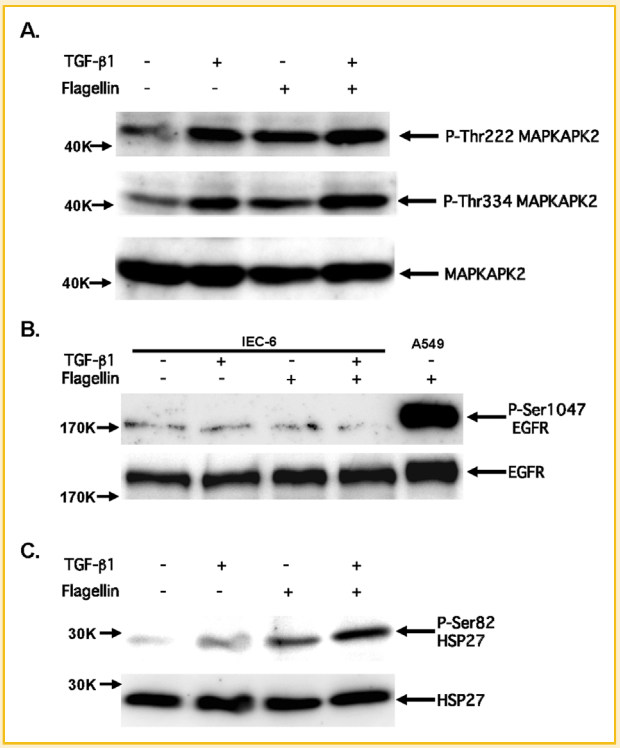

Fig. 3. Activation of mitogen-activated protein kinase-activated protein kinase-2 (MAPKAPK-2) and phosphorylation of epidermal growth factor receptor (EGFR) and heat shock protein 27 (HSP27) by transforming growth factor beta 1 (TGF-β1) and flagellin. A: IEC-6 cells were treated with 10 ng/ml TGF-β1, 2 μg/ml flagellin, or both TGF-β1 and flagellin for 30 min. The cell extracts (39.8 μg) were subjected to SDS-PAGE in 10% (wt/vol) acrylamide, and immunoblotting analysis was performed with an anti-P-Thr222 MAPKAPK-2 antibody (1:750) or an anti-P-Thr334 MAPKAPK-2 antibody (1:750). After the anti-P-Thr334 MAPKAPK-2 antibody was stripped off, immunoblotting with an anti-MAPKAPK-2 antibody was performed at a dilution of 1:750. The bands for MAPKAPK-2 (P-Thr222 MAPKAPK2, P-Thr334 MAPKAPK2, and MAPKAPK2) are indicated. B: IEC-6 cells were treated as described above. The cell extracts (39.8 μg) were subjected to SDS-PAGE in 7.5% (wt/vol) acrylamide, and immunoblotting analysis was performed with an anti-P-Ser1047 EGFR antibody (1:100). After the anti-P-Ser1047 EGFR antibody was stripped off, immunoblotting with an anti-EGFR antibody (1:600) was performed. The cell extracts (39.8 μg) were also subjected to SDS-PAGE in 10% acrylamide, and immunoblotting analysis was performed with an anti-P-Ser82 HSP27 antibody (1:750). After the antibody was stripped off, immunoblotting with an anti-HSP27 antibody was performed at a dilution of 1:750. The bands for EGFR (P-Ser1047 EGFR and EGFR) and HSP27 (P-Ser82 HSP27 and HSP27) are indicated.

ACTIVATION OF MAPKAPK-2 AND PHOSPHORYLATION OF HSP27 BY TGF-β1 AND FLAGELLIN

MAPKAPK-2 is activated by phosphorylation at multiple sites by p38 MAPK [Ben-Levy et al., 1995]. We found that flagellin treatment of A549 cells activated MAPKAPK-2 through activation of p38 MAPK [Noguchi et al., 2013]. In contrast, TGF-β1 did not activate MAPKAPK-2, although it activated p38 MAPK [Noguchi et al., 2013]. Therefore, we examined whether or not TGF-β1 and flagellin activated MAPKAPK-2 in IEC-6 cells. It has been reported that phosphorylation of any two of the residues Thr222, Ser272, and Thr334 was necessary and sufficient for maximal activation of MAPKAPK-2 [Ben-Levy et al., 1995]. In the present experiment, we examined the phosphorylation of Thr222 and Thr334 using available antibodies (Fig. 3A). We found that 30 min treatment with TGF-β1 and flagellin increased the phosphorylation of Thr222 by approximately 1.7- and 1.7-fold, respectively. Phosphorylation of Thr334 was increased by approximately 1.7- and 1.6-fold by TGF-β1 and flagellin, respectively. In addition, TGF-β1 plus flagellin increased the phosphorylation of Thr222 and Thr334 by approximately 2.2- and 2.9-fold, respectively. These results suggested that p38 MAPK, which was activated in an additive fashion by TGF-β1 and flagellin (Fig. 2A), also activated MAPKAPK-2 in an additive fashion.

Next, we examined phosphorylation of the physiological substrates of MAPKAPK-2, including HSP27 [Rouse et al., 1994]. In our previous study, we reported that purified MAPKAPK-2 phosphorylated EGFR at Ser1047 in vitro [Noguchi et al., 2013]. Previously, we also found that flagellin treatment of A549 cells increased the phosphorylation of EGFR at Ser1047, and that both inhibitors of p38 MAPK and MAPKAPK-2 inhibited phosphorylation [Noguchi et al., 2013]. These results strongly suggested that EGFR

was phosphorylated by MAPKAPK-2 in A549 cells. Therefore, we examined the phosphorylation of EGFR in IEC-6 cells. We confirmed that EGFR was phosphorylated at Ser1047 after treatment of A549 cells with flagellin (Fig. 3B). We found that EGFR protein level in IEC-6 cells were about 60% of that in A549 cells (Fig. 3B). Neither TGF-β1 nor flagellin increased the phosphorylation of EGFR at Ser1047, and the phosphorylation level in IEC-6 cells was much weaker than that in A549 cells (Fig. 3B). In addition, we examined the phosphorylation of HSP27. We found that the phosphorylation of HSP27 was increased by approximately 1.8- and 2.4-fold by TGF-β1 and flagellin, respectively (Fig. 3B). In addition, TGF-β1 plus flagellin increased phosphorylation by approximately 3.2-fold. These results suggested that phosphorylation of HSP27 was regulated by both flagellin and TGF-β1 in IEC-6 cells.

INDUCTION OF EMT-RELATED CHANGES BY TGF-β1 AND FLAGELLIN

TGF-β1 has been reported to increase the protein levels of fibronectin and reduce that of E-cadherin in pulmonary epithelial 1HAEo$^-$ cells [Kolosova et al., 2011]. We found that flagellin, as well as TGF-β1, increased the protein levels of fibronectin and reduced those of E-cadherin in A549 cells [Kondo et al., 2012]. These results suggested that flagellin induced EMT-related changes in alveolar epithelial cells in collaboration with TGF-β1. Therefore, we next examined whether or not flagellin induced the biochemical signs of EMT in IEC-6 cells. We found that neither TGF-β1 nor flagellin reduced the level of E-cadherin protein after 48 h of treatment (Fig. 4A). In the presence of both TGF-β1 and flagellin, E-cadherin protein level was reduced to about 70% of the control value. After 72 h of treatment, TGF-β1 and flagellin reduced E-cadherin protein level to about 75 and 70%, respectively, of the control value, but no additive effect of TGF-β1 and flagellin was observed. These results suggested that the effects of TGF-β1 and flagellin on E-cadherin protein level in IEC-6 cells were not so strong. TGF-β1 increased the level of fibronectin protein by approximately 2.2-fold and 1.7-fold, after 48 h and 72 h, respectively, of treatment. In contrast, flagellin did not increase the level of fibronectin protein, or enhance the effects of TGF-β1. In A549 cells, αSMA was not induced by TGF-β1 or flagellin [Kondo et al., 2012]. However, TGF-β1 dramatically increased the level of αSMA protein in IEC-6 cells (Fig. 4A). Flagellin alone increased the level of αSMA only slightly, but enhanced the effect of TGF-β1. TGF-β1, flagellin, and TGF-β1 with flagellin increased the level of αSMA by approximately 13.5-, 1.9-, and 23.2-fold, respectively, after 72 h of treatment. When an antibody against GAPDH was used for immunoblotting, no significant change in immunoreactivity was observed for any treatment (Fig. 4A). Microscopic examination did not show the clear morphological changes of EMT after 72 h of treatment with TGF-β1, flagellin, or TGF-β1 plus flagellin (data not shown).

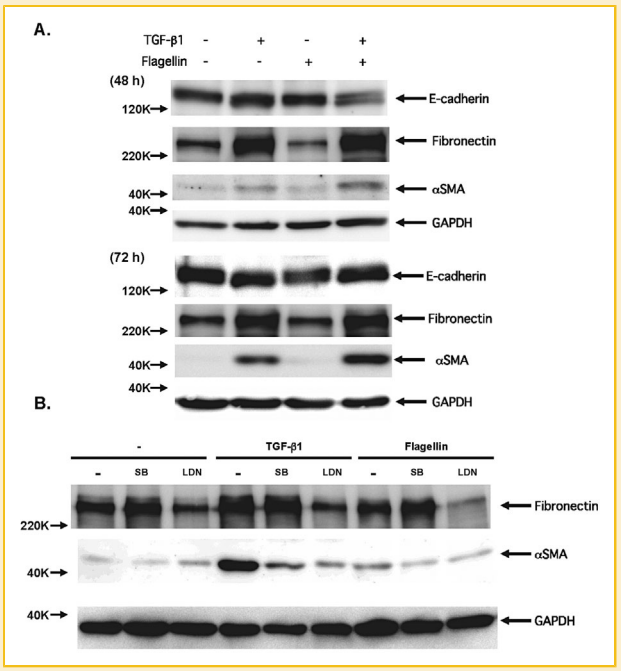

Fig. 4. Effects of transforming growth factor beta 1 (TGF-β1) and flagellin on epithelial-mesenchymal transition (EMT)-related changes in protein expression. A: IEC-6 cells were treated with 10 ng/ml TGF-β1, 2 μg/ml flagellin, or both TGF-β1 and flagellin for 48 or 72 h. The cell extracts (16.5 μg) were subjected to SDS-PAGE in 7.5% (wt/vol) acrylamide, and immunoblotting analysis was performed with an anti-E-cadherin antibody (1:750). After the anti-E-cadherin antibody was stripped off, immunoblotting with an anti-fibronectin antibody was performed at a dilution of 1:500. The cell extracts (16.5 μg) were also subjected to SDS–PAGE in 12% acrylamide, and immunoblotting analysis was performed with an anti-α-smooth muscle actin (αSMA) antibody (1:500) or an anti-glyceraldehyde-3-phosphate dehydrogenase (GAPDH) antibody (1:2,000). B: IEC-6 cells were pretreated with or without 5 μM SB203580 (SB) or 2 μM LDN193189 (LDN) for 30 min, and treated with 10 ng/ml TGF-β1, 2 μg/ml flagellin, or both TGF-β1 and flagellin for 48 h. The cell extracts (25.5 μg) were subjected to SDS–PAGE in 7.5% (wt/vol) acrylamide, and immunoblotting analysis was performed with an anti-fibronectin antibody (1:500). The cell extracts (25.5 μg) were also subjected to SDS–PAGE in 12% acrylamide, and immunoblotting analysis was performed with an anti-αSMA antibody (1:500). After the anti-αSMA antibody was stripped off, immunoblotting with an anti-GAPDH antibody was performed at a dilution of 1:2,000. The bands for E-cadherin, fibronectin, αSMA, and GAPDH are indicated.

INVOLVEMENT OF THE p38 MAPK AND SMAD PATHWAYS IN THE INDUCTION OF FIBRONECTIN AND αSMA

We next examined whether the SMAD pathway or the p38 MAPK pathway was involved in the induction of fibronectin and αSMA (Fig. 4B). SB203580, an inhibitor of p38 MAPK, did not inhibit the TGF-β1-induced increase in the level of fibronectin, whereas LDN193189, an inhibitor of the SMAD pathway, inhibited it by 51.7%. These results suggested that SMAD pathway was necessary for the induction of fibronectin. We noticed that LDN193189, but not SB203580, reduced the level of fibronectin by 36.8% in the absence of TGF-β1. This might suggest that the SMAD pathway was slightly activated and kept the protein level of fibronectin under basal conditions. In addition, 10 μM of ALK5 inhibitor inhibited fibronectin protein level by 22% and 57% in the absence and presence of TGF-β1, respectively (data not shown). Five μM of SIS3, an inhibitor of SMAD3 phosphorylation, inhibited fibronectin protein level by 11% and 44% in the absence and presence of TGF-β1, respectively. Both SB203580 and LDN193189 inhibited the TGF-β1-induced increase in the level of αSMA protein (Fig. 4B). These results suggested that both the p38 MAPK and SMAD

pathways were necessary for the induction of αSMA. ALK5 inhibitor and SIS3 did not reduce αSMA protein level in the presence of TGF-β1 (data not shown). These results may suggest that ALK5 and SMAD3 were not involved in the induction of αSMA. In Figure 4B, flagellin alone increased the level of αSMA protein, and SB203580 inhibited the effect of flagellin.

STIMULATION OF MIGRATION BY TGF-β1 AND FLAGELLIN

It is well known that TGF-β1 stimulates the migration of various cultured cells [Lavoie et al., 1993]. In addition, it has been reported that p38 MAPK is involved in this response to TGF-β1 [Lavoie et al., 1993]. Because TGF-β1 and flagellin activated p38 MAPK in IEC-6 cells, we examined whether TGF-β1 or flagellin stimulated migration using a wound healing assay (Fig. 5). The addition of TGF-β1 or flagellin stimulated wound closure strongly after 16 h of treatment, and no wound was observed in the presence of TGF-β1 plus flagellin (Fig. 5A). When each initial wound area was taken as 100%, the remaining wound was $39.9 \pm 3.3\%$ in the absence of TGF-β1 and flagellin, and $17.5 \pm 6.8\%$ ($P < 0.01$), $13.4 \pm 4.7\%$ ($P < 0.01$), and $0.1 \pm 0.1\%$ ($P < 0.01$) in the presence of TGF-β1, flagellin, and TGF-β1 plus flagellin, respectively (Fig. 5B). After 24 h of treatment, essentially no wound was observed in the presence of TGF-β1 or flagellin, whereas the remaining wound was $20.6 \pm 3.2\%$ in the absence of TGF-β1 and flagellin (Fig. 5B).

EFFECTS OF FLAGELLIN AND TGF-β1 ON THE GROWTH OF IEC-6 CELLS

We next examined whether flagellin or TGF-β1 affected the growth of IEC-6 cells. We took the cell number as 100% when we seeded the cells at 10,000 cells/well and cultured for 24 h in 0.1% FCS. In these conditions, the cell number was $42.2 \pm 9.5\%$ and $12.1 \pm 1.0\%$, when the cells were seeded at 5,000 and 1,000 cells/well, respectively. No stimulation of cell growth was observed with TGF-β1 or flagellin. These results strongly suggested that the stimulation of wound closure by flagellin and TGF-β1 was not due to the stimulation of cell growth.

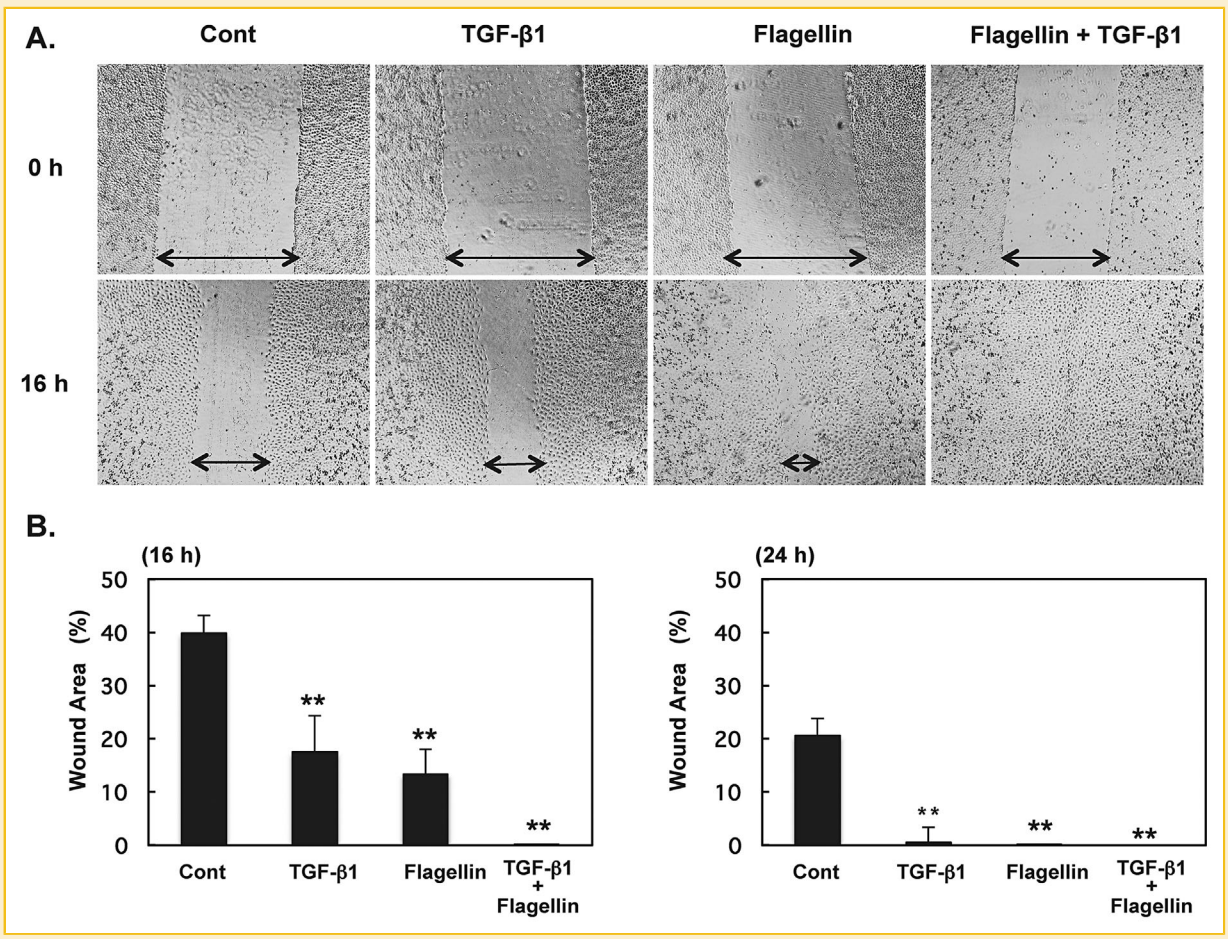

Fig. 5. Effects of transforming growth factor beta 1 (TGF-β1) and flagellin on wound healing. A: IEC-6 cells were seeded and cultured in 24-well plates as described in the Materials and Methods. Wound healing was examined after treatment with 10 ng/ml TGF-β1, 2 μg/ml flagellin, or both TGF-β1 and flagellin for 16 h. Phase contrast microscopy images of the cells were taken at 0 h and 16 h. The width of each wound is indicated. B: Each initial wound area was taken as 100%, and wound healing was estimated as a percentage of the remaining wound area relative to each initial wound area after 16 h and 24 h, as indicated. Values are the mean ± SE (four samples per condition from two different experiments). $^{**}P < 0.01$ (vs. control).

INVOLVEMENT OF P38 MAPK IN THE STIMULATION OF MIGRATION BY FLAGELLIN

Because p38 MAPK was reported to be involved in the stimulation of migration by TGF-β1 in cultured mammary epithelial cells [Bakin et al., 2002], we examined whether or not p38 MAPK was involved in the flagellin-induced migration of IEC-6 cells (Fig. 6). In this study, the remaining wound was $64.0 \pm 0.8\%$ after 16 h of culture in the absence of flagellin. SB203580 alone had no effect on wound closure, and the remaining wound was $63.9 \pm 2.2\%$. Flagellin reduced the remaining wound to $36.5 \pm 3.2\%$ ($P < 0.01$). It was of interest that wound closure in response to flagellin was completely inhibited by SB203580, and the remaining wound was $56.9 \pm 3.5\%$. The inhibitory effects of SB203580 were observed also after 24 h of culture. The remaining wound was $44.5 \pm 1.5\%$, $44.7 \pm 1.4\%$, $12.9 \pm 0.3\%$ ($P < 0.01$), and $39.3 \pm 5.0\%$, in the absence of flagellin and SB203580, in the presence of SB203580 alone, flagellin alone, and SB203580 plus flagellin, respectively. These results suggested that p38 MAPK was necessary for the flagellin-stimulated migration of IEC-6 cells.

INVOLVEMENT OF MAPKAPK-2 IN THE STIMULATION OF MIGRATION BY FLAGELLIN

We next examined whether or not MK2a inhibitor, an inhibitor of MAPKAPK-2, inhibited the flagellin-induced migration of IEC-6 cells (Fig. 7). In this study, the remaining wound was $37.4 \pm 4.5\%$ after 16 h of culture in the absence of flagellin. MK2a inhibitor alone had no effect on wound closure, and the remaining wound was $39.5 \pm 1.8\%$. Flagellin reduced the remaining wound to $10.3 \pm 1.6\%$ ($P < 0.05$). It was of interest that wound closure in response to flagellin was completely inhibited by MK2a inhibitor, and the remaining wound was $35.8 \pm 1.4\%$. After 24 h of culture, the remaining wound was $18.9 \pm 4.0\%$, $22.6 \pm 1.5\%$, $3.6 \pm 1.9\%$ ($P < 0.05$), and $24.4 \pm 3.0\%$, in the absence of flagellin and MK2a inhibitor, in the presence of MK2a inhibitor alone, flagellin alone,

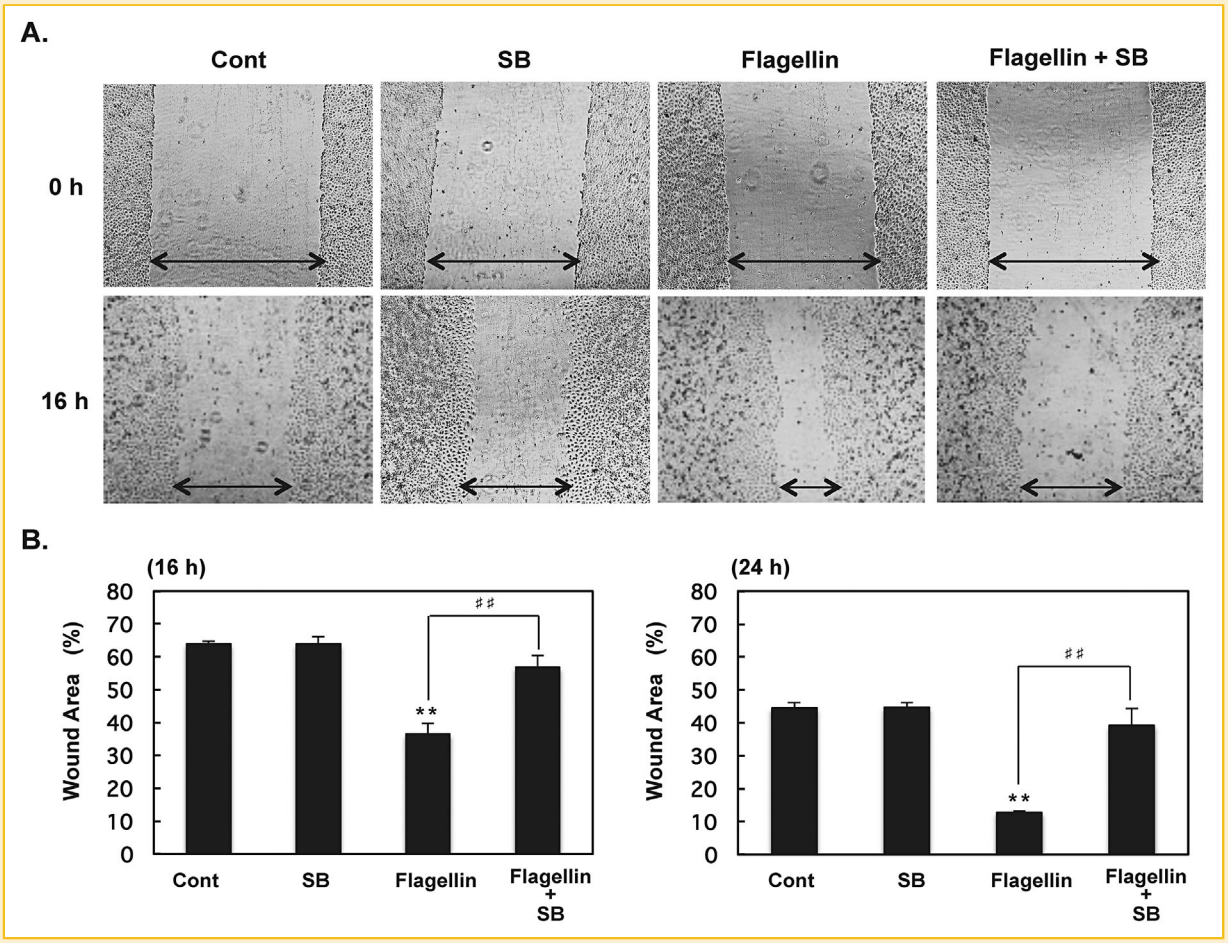

Fig. 6. Effect of SB203580 (SB) on flagellin-induced wound healing. A: IEC-6 cells were seeded and cultured in 24-well plates as described in the Materials and Methods. Wound healing was examined after treatment with 5 μM SB203580, 2 μg/ml flagellin, or both SB203580 and flagellin for 16 h. Phase contrast microscopy images of the cells were taken at 0 h and 16 h. The width of each wound is indicated. B: Each initial wound area was taken as 100%, and wound healing was estimated as a percentage of the remaining wound area relative to each initial wound area after 16 h and 24 h, as indicated. Values are the mean ± SE (four samples per condition from two different experiments). $^{**}P < 0.01$ (vs. control). The difference in wound area between cells treated with flagellin and those treated with both flagellin and SB203580 was statistically significant ($P < 0.01$).

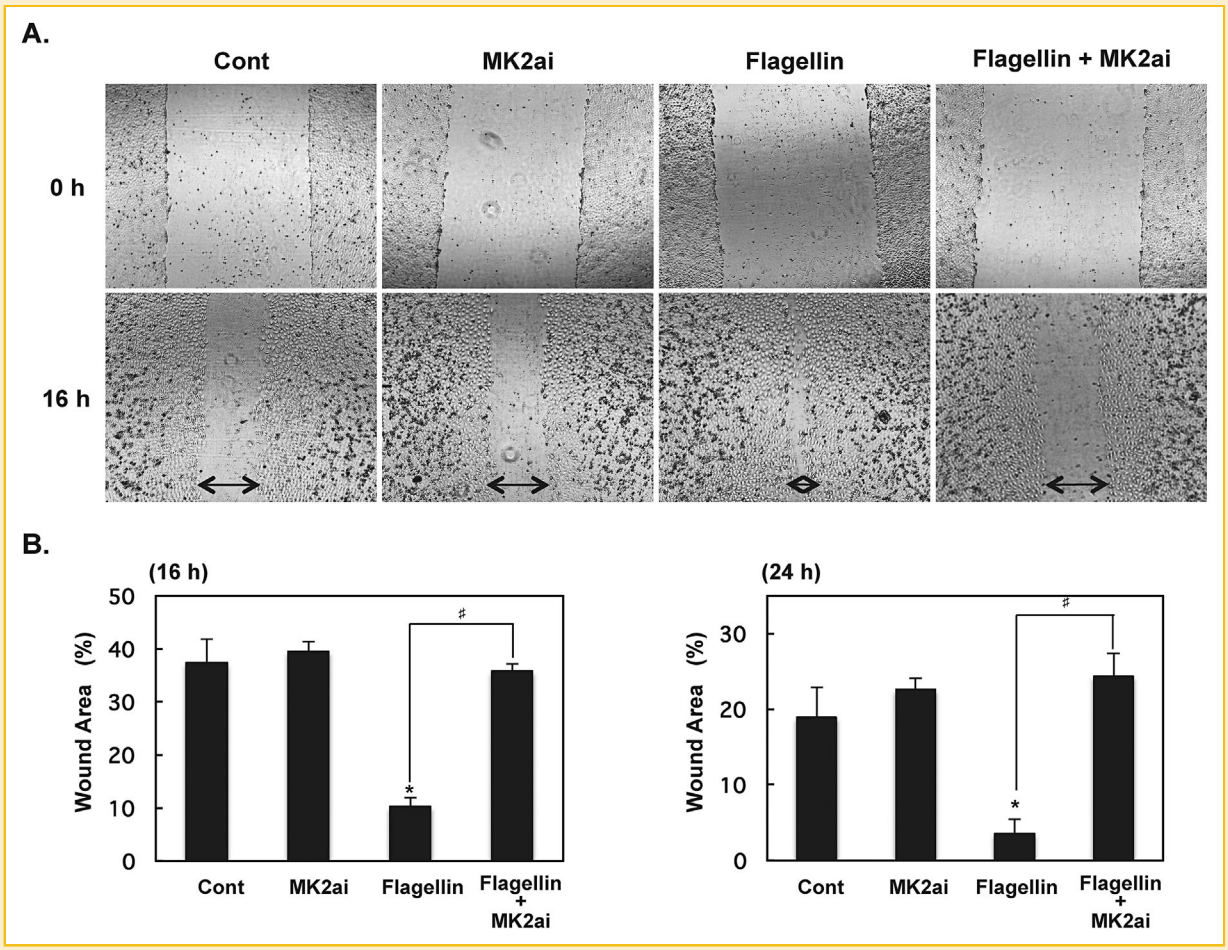

Fig. 7. Effect of MK2a inhibitor on flagellin-induced wound healing. A: IEC-6 cells were seeded and cultured in 24-well plates as described in the Materials and Methods. Wound healing was examined after treatment with 20 μM MK2a inhibitor (MK2ai), 2 μg/ml flagellin, or both MK2a inhibitor and flagellin for 16 h. Phase contrast microscopy images of the cells were taken at 0 h and 16 h. The width of each wound is indicated. *B*: Each initial wound area was taken as 100%, and wound healing was estimated as a percentage of the remaining wound area relative to each initial wound area after 16 h and 24 h, as indicated. Values are the mean ± SE (four samples per condition from two different experiments). $^{*}P < 0.05$ (vs. control). The difference in wound area between cells treated with flagellin and those treated with both flagellin and MK2a inhibitor was statistically significant ($P < 0.05$).

and MK2a inhibitor plus flagellin, respectively (Fig. 7B). These results suggested that MAPKAPK-2 was necessary for the flagellin-stimulated migration of IEC-6 cells.

EFFECTS OF TGF-β1 AND FLAGELLIN ON THE PHOSPHORYLATION OF HSP27 IN A549 CELLS AND CELLULAR MIGRATION

Finally, we examined whether treatment of A549 cells with TGF-β1 or flagellin induced the phosphorylation of HSP27 and stimulated cell migration (Fig. 8). We found that the phosphorylation of HSP27 was increased by approximately 1.5- and 3.3-fold by TGF-β1 and flagellin, respectively (Fig. 8A). In addition, TGF-β1 plus flagellin increased HSP27 phosphorylation by approximately 4.4-fold. These results suggested that phosphorylation of HSP27 was regulated by both TGF-β1 and flagellin in A549 cells as well as IEC-6 cells.

Compared with IEC-6 cells, the migration of A549 cells was less remarkable, and the remaining wound was 72.3 ± 2.2% and 61.5 ± 2.6% after 24 h and 48 h of culture, respectively, in the absence of TGF-β1 and flagellin (Fig. 8B). Addition of TGF-β1 significantly stimulated wound closure, and the remaining wound after 24 h and 48 h was 40.3 ± 3.1% ($P < 0.05$) and 36.3 ± 3.2% ($P < 0.01$), respectively. In contrast, no significant stimulation of cell migration by flagellin was observed, and the remaining wound after 24 h and 48 h was 64.7 ± 1.8% and 57.4 ± 2.3%, respectively. In addition, flagellin did not enhance the migration effect of TGF-β1. These results suggested that the stimulation of TLR5 in A549 cells did not induce cell migration, although it increased the phosphorylation of HSP27.

DISCUSSION

Infection by flagellated bacteria can occur in both the lung and intestine, and alveolar epithelial cells and intestinal epithelial cells express TLR5, which is a receptor for flagellin [Hayashi et al., 2001]. Stimulation of TLR5 is involved in innate immune responses [Rolli et al., 2010; Huebener and Schwabe, 2013]. Changes in cell functions

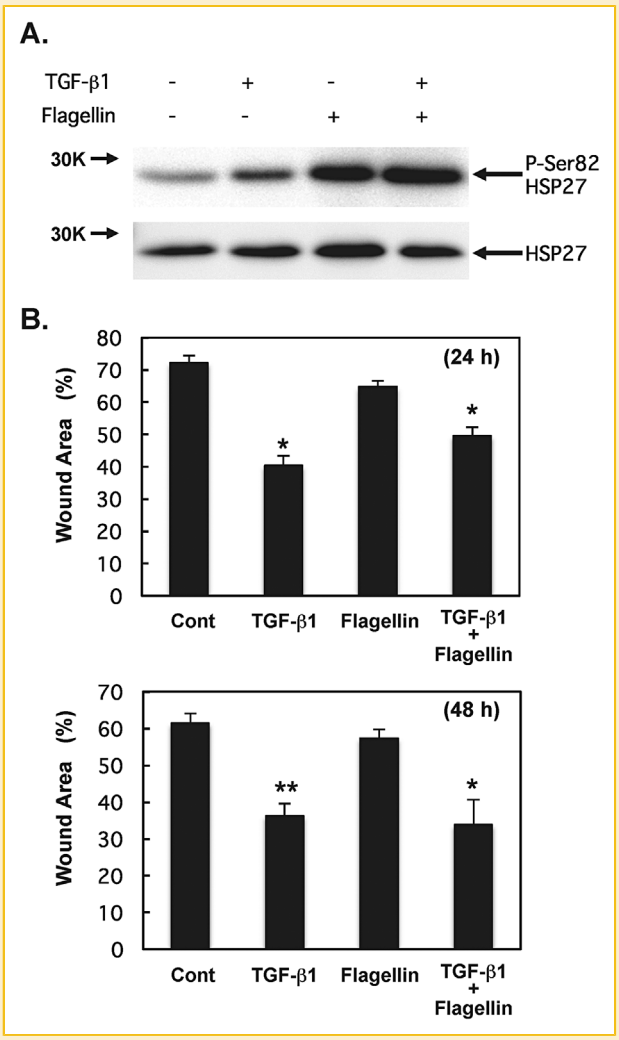

Fig. 8. Effects of transforming growth factor beta 1 (TGF-β1) and flagellin on phosphorylation of heat shock protein 27 (HSP27) and wound healing. A: A549 cells were treated with 10 ng/ml TGF-β1, 2 μg/ml flagellin, or both TGF-β1 and flagellin for 30 min. The cell extracts (42 μg) were subjected to SDS–PAGE in 10% (wt/vol) acrylamide, and immunoblotting analysis was performed with an anti-P-Ser82 HSP27 antibody (1:750). After the antibody was stripped off, immunoblotting with an anti-HSP27 antibody was performed at a dilution of 1:750. The bands for HSP27 (P-Ser82 HSP27 and HSP27) are indicated. B: A549 cells were seeded and cultured in 24-well plates as described in the Materials and Methods. Wound healing was examined after treatment with 10 ng/ml TGF-β1, 2 μg/ml flagellin, or both TGF-β1 and flagellin for 48 h. Phase contrast microscopy images of the cells were taken at 0 h, 24 h, and 48 h. Each initial wound area was taken as 100%, and wound healing was estimated as a percentage of the remaining wound area relative to each initial wound area after 24 h and 48 h, as indicated. Values are the mean ± SE (four samples per condition from two different experiments). $^{**}P < 0.01$; $^{*}P < 0.05$ (vs. control).

other than the innate immune responses by stimulation of TLR5 in the intestine are not fully understood at present. In our previous study, we found that TLR5 stimulation of cultured alveolar epithelial cells activated the p38 MAPK pathway as well as the NF-κB pathway [Kondo et al., 2012]. In the present study, we first confirmed that TLR5 stimulation of cultured intestinal epithelial cells, IEC-6 cells, activated the NF-κB pathway and the p38 MAPK pathway. In contrast, TGF-β1 activated the SMAD pathway and the p38 MAPK pathway. These results indicated that TLR5 and TGF-β family receptors activated distinct pathways (NF-κB pathway or SMAD pathway) and a common pathway (p38 MAPK pathway) to control the functions of IEC-6 cells. We then focused on changes in cell functions, such as cell migration, through the p38 MAPK pathway. The roles of activation of the NF-κB pathway in the migration of IEC-6 cells are not clear at present and should be an important focus for a future study.

Overstimulation of TLR5 in intestinal epithelial cells by commensal gut bacteria has been reported to be the cause of CD [Lodes et al., 2004]. Using cultured alveolar epithelial cells, we found that TLR5 stimulation induced EMT-like changes [Kondo et al., 2012]. Because one of the major complications of CD is intestinal fibrosis, we considered the possibility that TLR5 stimulation in intestinal epithelial cells might induce EMT-like changes, leading to intestinal fibrosis. Therefore, we examined whether or not TLR5 stimulation of IEC-6 cells induced EMT-like changes. From our previous findings with cultured alveolar epithelial cells [Kondo et al., 2012], we expected that treatment of IEC-6 cells with flagellin would induce EMT-like changes through activation of the p38 MAPK pathway. However, treatment of IEC-6 cells with TGF-β1 and flagellin did not induce EMT-like morphological changes. Instead, we found that TGF-β1 and flagellin remarkably stimulated the migration of IEC-6 cells in a wound healing assay.

It has been reported that flagellin promoted the migration of salivary gland adenocarcinoma cell lines [Park et al., 2015] and oral and cutaneous squamous cell carcinoma cells [Ahmed Haji Omar et al., 2015]. These effects of flagellin may be related to tumor progression and metastasis [Park et al., 2011; Ahmed Haji Omar et al., 2015]. In addition, the stimulation of migration of intestinal epithelial cells could accelerate wound healing for the reconstruction of intestinal epithelia after inflammation. Impairment of wound healing may induce a number of complications, including fistula formation in the case of CD.

We found that cell migration was stimulated by TGF-β1 and flagellin without a reduction in E-cadherin protein level. If migration of IEC-6 cells was sheet-motility instead of amboid or single cell, a reduction of E-cadherin may not be necessary for cell migration [for review, see Ref. Friedl et al., 2014]. It may also be possible that the localization of E-cadherin was altered to allow the cells separate easily. Immunocytochemical examination of changes in the localization of E-cadherin after flagellin treatment will be of interest for a future study.

In translating our findings in IEC-6 cells to alveolar epithelial cells, we intended to examine whether or not flagellin stimulated the migration of cultured alveolar epithelial cells. In our previous studies, we examined the effects of flagellin on EMT and regulation of EGFR using various types of cultured alveolar epithelial cells [Kondo et al., 2012; Noguchi et al., 2013; Nishi et al., 2015]. We found that A549 cells were the most suitable for examining the molecular mechanisms of flagellin effects [Kondo et al., 2012; Nishi et al., 2015]. Therefore, we decided to use A549 cells to examine the effects of flagellin on the phosphorylation of HSP27 and cell migration. HSP27 was phosphorylated after flagellin treatment of A549 cells, whereas no stimulatory effects of flagellin on cell

migration were observed. These results suggested that changes in cell functions caused by TLR5 stimulation were different between alveolar epithelial cells and intestinal epithelial cells. It is unlikely that any compounds in the culture medium or methods for coating of dishes caused the different cell responses, because we cultured and treated IEC-6 cells and A549 cells under exactly the same conditions. The signal transduction mechanisms after stimulation of the p38 MAPK pathway should be examined to compare A549 cells and IEC-6 cells in a future study.

Our inhibitor studies strongly suggested that MAPKAPK-2 activated by p38 MAPK was involved in the stimulation of migration of IEC-6 cells by flagellin (Figs. 6 and 7). We also found additive effects of flagellin and TGF-β1 on activation of MAPKAPK-2 and migration (Figs. 3A and 5), which further supported our idea that migration was stimulated through the activation of MAPKAPK-2.

The molecular mechanisms by which MAPKAPK-2 stimulates migration are not clear at present. It has been reported that HSP27 is enriched at the leading edge of polarized fibroblasts, and that HSP27 regulates actin polymerization [Miron et al., 1991]. It was also reported that phosphorylation of HSP27 induced the accumulation of cortical F-actin at the leading edge [Lavoie et al., 1993]. We found that phosphorylation of HSP27 was increased after flagellin treatment. In addition, it has already been reported that phosphorylation of HSP27 by MAPKAPK-2 activated by p38 MAPK stimulated migration of macrophages, fibroblasts, and glioma cells [Rousseau et al., 2006; Alam et al., 2013]. Taken together, it is possible that MAPKAPK-2 stimulates migration of IEC-6 cells via the phosphorylation of HSP27. In contrast, we also found that treatment of A549 cells with TGF-β1 and flagellin increased the phosphorylation of HSP27. However, flagellin did not stimulate the migration of A549 cells. In addition, we found recently that MK2a inhibitor did not significantly inhibit the phosphorylation of HSP27 (Kondo et al., unpublished observation). Therefore, unknown substrate proteins for MAPKAPK-2 other than HSP27 may be involved in the flagellin-induced migration of IEC-6 cells.

In the present study, we used flagellin purified from *B. subtilis* to stimulate TLR5. Because the amino acids crucial for TLR5 recognition are conserved among *B. subtilis,* commensal gut bacteria, and entero-invasive bacteria such as *Vibrio cholera* [Smith et al., 2003], it is highly possible that flagellin from enterobacteria, as well as *B. subtilis*, stimulates TLR5 in intestinal epithelial cells.

ACKNOWLEDGMENTS

We gratefully acknowledge Dr. Y. Isohama (Tokyo University of Science) for kindly providing A549 cells. This work was supported by JSPS KAKENHI Grant Numbers 23500451, 24700381, 23390376, and 725293329. We thank the Research Laboratory Center of Faculty of Medicine, University of the Ryukyus for technical support.

REFERENCES

Akira S. 2003. Toll-like receptor signaling. J Biol Chem 278:38105–38108.

Ahmed Haji Omar A, Korvala J, Haglund C, Virolainen S, Hayry V, Atula T, Kontio R, Rihtniemi J, Pihakari A, Sorsa T, Hagstrom J, Salo T. 2015. Toll-like receptors -4 and -5 in oral and cutaneous squamous cell carcinomas. J Oral Pathol Med 44:258–265.

Alam R, Schultz CR, Golembieski WA, Poisson LM, Rempel SA. 2013. PTEN suppresses SPARC-induced pMAPKAPK2 and inhibits SPARC-induced Ser78 HSP27 phosphorylation in glioma. Neuro Oncol 15:451–461.

Bakin AV, Rinehart C, Tomlinson AK, Arteaga CL. 2002. P38 mitogen-activated protein kinase is required for TGFb-mediated fibroblastic trans-differentiation and cell migration. J Cell Sci 115:3193–3206.

Ben-Levy R, Leighton IA, Doza YN, Attwood P, Morrice N, Marshall CJ, Cohen P. 1995. Identification of novel phosphorylation sites required for activation of MAPKAP kinase-2. EMBO J 14:5920–5930.

Flier SN, Tanjore H, Kokkotou EG, Sugimoto H, Zeisberg M, Kalluri R. 2010. Identification of epithelial to mesenchymal transition as a novel source of fibroblasts in intestinal fibrosis. J Biol Chem 285:20202–20212.

Friedl P, Wolf K, Zegers MM. 2014. Rho-directed forces in collective migration. Nat Cell Biol 16:208–210.

Harrison LM, Rallabhandi P, Michalski J, Zhou X, Steyert SR, Vogel SN, Kaper JB. 2008. *Vibrio cholerae* flagellins induce Toll-like receptor 5-mediated interleukin-8 production through mitogen-activated protein kinase and NF-kB activation. Infect Immun 76:5524–5534.

Hayashi F, Smith KD, Ozinsky A, Hawn TR, Yi EC, Goodlett DR, Eng JK, Akira S, Underhill DM, Aderem A. 2001. The innate immune response to bacteria flagellin is mediated by Toll-like receptor 5. Nature 410:1099–1103.

Higa-Nakamine S, Maeda N, Toku S, Yamamoto T, Yingyuenyong M, Kawahara M, Yamamoto H. 2012. Selective cleavage of ErbB4 by G-protein-coupled gonadotropin-releasing hormone receptor in cultured hypothalamic neurons. J Cell Physiol 227:2492–2501.

Huebener P, Schwabe RF. 2013. Regulation of wound healing and organ fibrosis by toll-like receptors. Biochim Biophys Acta 1832:1005–1017.

Kolosova I, Nethery D, Kern JA. 2011. Role of Smad2/3 and p38 MAP kinase in TGF-b1-induced epithelial-mesenchymal transition of pulmonary epithelial cells. J Cell Physiol 226:1248–1254.

Kondo Y, Higa-Nakamine S, Noguchi N, Maeda N, Toku S, Isohama Y, Sugahara K, Kukita I, Yamamoto H. 2012. Induction of epithelial-mesenchymal transition by flagellin in cultured lung epithelial cells. Am J Physiol Lung Cell Mol Physiol 303:L1057–L1069.

Laemmli UK. 1970. Cleavage of structural proteins during the assembly of the head of bacteriophage T4. Nature 227:680–685.

Lavoie JN, Hickey E, Weber LA, Landry J. 1993. Modulation of actin microfilament dynamics and fluid phase pinocytosis by phosphorylation of heat shock protein 27. J Biol Chem 268:24210–24214.

Lodes MJ, Cong Y, Elson CO, Mohamath R, Landers CJ, Targan SR, Fort M, Hershberg RM. 2004. Bacterial flagellin is a dominant antigen in Crohn disease. J Clin Invest 113:1296–1306.

Miron T, Vancompernolle K, Vandekerckhove J, Wilchek M, Geiger B. 1991. A 25-kD inhibitor of actin polymerization is a low molecular mass heat shock protein. J Cell Biol 114:255–261.

Mizutani A, Maeda N, Toku S, Isohama Y, Sugahara K, Yamamoto H. 2010. Inhibition by ethyl pyruvate of the nuclear translocation of nuclear factor-kB in cultured lung epithelial cells. Pulm Pharmacol Ther 23:308–315.

Newton HJ, Ang DK, van Driel IR, Hartland EL. 2010. Molecular pathogenesis of infections caused by *Legionella pneumophila.* Clin Microbiol Rev 23:274–298.

Nishi H, Maeda N, Izumi S, Higa-Nakamine S, Toku S, Kakinohana M, Sugahara K, Yamamoto H. 2015. Differential regulation of epidermal growth factor receptor by hydrogen peroxide and flagellin in cultured lung alveolar epithelial cells. Eur J Pharmacol 748:133–142.

Noguchi N, Kondo Y, Maeda N, Higa-Nakamine S, Toku S, Maruyama J, Isohama Y, Kukita I, Sugahara K, Yamamoto H. 2013. Phosphorylation of epidermal growth factor receptor at serine 1047 by MAP kinase-activated protein kinase-2 in cultured lung epithelial cells treated with flagellin. Arch Biochem Biophys 529:75–85.

Park J-H, Yoon H-F, Kim D-J, Kim S-A, Ahn S-G, Yoon J-H. 2011. Toll-like receptor 5 activation promotes migration and invasion of salivary gland adenocarcinoma. J Oral Pathol Med 40:187–193.

Rolli J, Loukili N, Levrand S, Rosenblatt-Velin N, Rignault-Clerc S, Waeber B, Feihl F, Pacher P, Liaudet L. 2010. Bacterial flagellin elicits widespread innate immune defense mechanisms, apoptotic signaling, and a sepsis-like systemic inflammatory response in mice. Crit Care 14:R160.

Rouse J, Cohen P, Trigon S, Morange M, Alonso-Llamazares A, Zamanillo D, Hunt T, Nebreda AR. 1994. A novel kinase cascade triggered by stress and heat shock that stimulates MAPKAP kinase-2 and phosphorylation of the small heat shock proteins. Cell 78:1027–1037.

Rousseau S, Dolado I, Beardmore V, Shpiro N, Marqez R, Nebreda AR, Arthur JSC, Case LM, Tessier-Lavigne M, Gaestel M, Cuenda A, Cohen P. 2006. CXCL12 and C5a trigger cell migration via a PAK1/2-p38a MAPK-MAPKAP-K2-HSP27 pathway. Cell Signal 18:1897–1905.

Sierro F, Dubois B, Coste A, Kaiserlian D, Kraehenbuhl JP, Sirard JC. 2001. Flagellin stimulation of intestinal epithelial cells triggers CCL20-mediated migration of dendritic cells. Proc Natl Acad Sci USA 98:21–30.

Smith KD, Andersen-Nissen E, Hayashi F, Strobe K, Bergman MA, Barrett SL, Cookson BT, Aderem A. 2003. Toll-like receptor 5 recognizes a conserved site on flagellin required for protofilament formation and bacterial motility. Nature Immun 4:1247–1253.

Sun J, Fegan PE, Desai AS, Madara JL, Hobert ME. 2007. Flagellin-induced tolerance of the Toll-like receptor 5 signaling pathway in polarized intestinal epithelial cells. Am J Physiol Gastrointest Liver Physiol 292:G767–G778.

Towbin H, Staehelin T, Gordon J. 1979. Electrophoretic transfer of proteins from polyacrylamide gels to nitrocellulose sheets: procedure and some applications. Proc Natl Acad Sci USA 76:4350–4354.

Yamanaka A, Hiragami Y, Maeda N, Toku S, Kawahara M, Naito Y, Yamamoto H. 2007. Involvement of CaM kinase II in gonadotropin-releasing hormone-induced activation of MAP kinase in cultured hypothalamic neurons. Arch Biochem Biophys 466:234–241.

Zeng H, Wu H, Sloane V, Jones R, Yu Y, Lin P, Gewirtz AT, Neish AS. 2006. Flagellin/TLR5 responses in epithelia reveal intertwined activation of inflammatory and apoptotic pathways. Am J Physiol Gastrointest Liver Physiol 290:G96–G108.